J. Mater. Environ. Sci. 7 (1) (2016) 244-258
ISSN : 2028-2508
CODEN: JMESC

Effect of some Benzimidazolone compounds on C38 steel corrosion in hydrochloric acid solution

Ismaily Alaoui Khadija[1], F. Ouazzani [2], Y. kandri rodi[2], A.M. Azaroual[3], Z. Rais [1], M. Filali Baba [1], M. Taleb[1], A. Chetouani[4;5], A. Aouniti[4], B. Hammouti[4]

[1]*Laboratoire d'Ingénierie d'Electrochimie de Modélisation et Environnement, LIEME Faculté des sciences Dhar El Mahraz Fès Maroc »*
[2]*Laboratoire de chimie organique appliqué LCOA Faculté des Sciences et technique Fès Maroc»*
[3]*Laboratoire des Matériaux, Electrochimie et Environnement, LMEE, Faculté des sciences Kenitra Maroc »*
[4]*Laboratoire de Chimie Appliquée et environnement (LCAE-URAC18), Faculté des Sciences, 60000 Oujda, Morocco.*
[5]*Laboratoire de chimie physique, Centre Régionale des Métiers de l'Education et de Formation "CRMEF", Région de l'Orientale, Oujda, Morocco*

Received 12 Mar 2015, Revised 17 Nov 2015, Accepted 29 Nov 2015
**For correspondence: Email:*

Abstract
The inhibitive action of some Benzimidazolone derivatives, namely 1, 3-dihydro-2H-benzimidazol-2-one (**BI_1**) and 1-(prop-2-en-1-yl)-1,3-dihydro-2H-benzimidazol-2-one (**BI_2**) against the corrosion of C38 steel in molar hydrochloric acid solution has been investigated using weight loss measurements, Tafel polarization and electrochemical impedance spectroscopy (EIS) techniques. Results obtained reveal that these derivatives perform excellently as corrosion inhibitors for mild steel in HCl 1M solution, its inhibiting efficiency reaches 92 % for BI_1 and 95% for BI_2 at 10^{-3} M. Polarization measurements showed that BI_1 is considered as an inhibitor of predominant anodic effect, but BI_2 act essentially as a mixed type inhibitor with anodic predominance at 10^{-3} M. The temperature effect on the corrosion behavior of mild steel in 1 M HCl with and without BI_1 and BI_2 at different concentrations was studied in the temperature range from 303 to 333 K. E% remains the same even at high temperature for BI1 and BI_2 at 10^{-3}M . The adsorption free energy and activation parameters for the mild steel dissolution reaction were determined. Both products are adsorbed on the mild steel surface according to a Langmuir isotherm adsorption model. Surface morphologies of sample were presented through scanning electron microscope (SEM).

Keywords: Corrosion inhibition; C38; Benzimidazolone ; Polarization curves; Adsorption process; Thermodynamic properties; SEM.

1. Introduction
Nowadays the study of carbon steel corrosion phenomena has become an important industrial and academic topic that has received a considerable amount of attention. Acid solutions are commonly used for the removal of undesirable scale and rust in the metal working, cleaning of boilers and heat exchangers. Hydrochloric acids are most widely used for all these purposes. However, the strong corrosivity of hydrochloric acid needs to be controlled by an appropriate corrosion inhibitor [1–4].
A perusal of literature [2-6] reveals that most of the efficient inhibitors used in industry are chemical compounds containing nitrogen, sulphur, oxygen with aromatic and heterocyclic rings through which induce greater adsorption of the inhibitor molecules onto the surface of mild steel [3–4] Furthermore, inhibitor adsorption is influenced by factors such as the nature and surface charges on the metal and the type of aggressive media, the structure of inhibitor, and the nature of its interaction with the metal surface. Among the

various nitrogenous compounds studied as inhibitors in our laboratory, several tetrazoles [6-7] pyridazines [8-9] pyrazoles [10] imidazoles [11] ….ect exhibit good inhibitory effect in molar hydrochloric acid [12]. Imidazole derivatives are well-known as corrosion inhibitors for metals and alloys [13-16-24]. Benzimidazolones molecules show to anchoring sites suitable for surface bonding [5]. Moreover planar benzimidazolone ring displays large projected area on metal surface and will show good inhibition effect.
This work is devoted to study the inhibition characteristics of 1, 3-dihydro-2H-benzimidazol-2-one (BI1) and 1-(prop-2-en-1-yl)-1,3-dihydro-2H-benzimidazol-2-one (BI2) for C38 steel in molar hydrochloric acid solution using weight loss, polarization and impedance methods. The effect of temperature on the inhibition efficiency was investigated and discussed.

2. Experimental part

2.1. Materials preparation

The structural formulas of the examined inhibitors in this study are shown in Fig. 1.

BI$_1$: 1,3-dihydro-2H-benzimidazol-2-one **BI$_2$**: 1-(prop-2-en-1-yl)-1,3-dihydro-2H- benzimidazol-2-one

Fig.1: Names and chemical structures of organic compounds studied

The aggressive medium (1M HCl), used as blank, was prepared by dilution of analytical grade 37% HCl with bi-distilled water. The C38 steel specimens having composition of (wt. %): 0.21 % C, 0.38 % Si, 0.05% Mn, 0.05% S, 0.09% P, 0.01 % Al and balance Fe) were used for gravimetric and electrochemical studies.

2.2. Weight loss measurements

Prior to experiment, specimens were mechanically polished successively with emery paper at different grit sizes (from 180 to 1200). Then, the specimens were cleaned with bi-distilled water then degreased with acetone and dried at room temperature. After weighing accurately, the specimens were immersed in 50 ml beaker, which contained 50 ml of 1M hydrochloric acid with and without addition of different concentrations of inhibitors. The steel specimens used had a rectangular form (2 cm x 1 cm x 0.25 cm). After 6 h, the specimens were taken out, washed, dried and weighed accurately. Then the tests were repeated at different temperatures.

2.3. Electrochemical measurement

Electrochemical measurements were earned out in a conventional three-electrode glass cell. The working electrode, in the form of a disc cut from steel, had a geometric area of 1 cm^2. KCl-saturated Ag/AgCl electrode and a platinum electrode were used as reference and auxiliary electrode, respectively. All tests were performed in continuously stirred conditions at room temperature. Potentiodynamic polarization experiments were recorded with a potentiostat of the type PGZ 100 and controlled with analysis software (Volta master 4). The polarization curves were recorded by changing the electrode potential automatically from −750 to -150 mV with

scanning rate of 1 mV/s. Before measurement, the working electrode was immersed in test solution at natural potential (open circuit potential) for 30 min until a steady state was reached. The linear Tafel segments, in a large domain of potential, of the cathodic curves were extrapolated to the corresponding corrosion potentials to obtain the corrosion current values.
Electrochemical impedance spectroscopy (EIS) measurements were carried out with a Volta lab PGZ 100 electrochemical system at E_{corr} after immersion in solution. After determination of the steady-state current at a given potential, sine wave voltage (10mV) peak to peak, at frequencies between 100 kHz and 10 mHz was superimposed on the rest potential. Computer programs automatically controlled the measurements performed at rest potentials after 30 min of exposure. EIS diagrams were given in the Nyquist representation.

2.4. Scanning electron microscope

SEM was used to observe the surface morphologies of specimens after 6h of immersion in 1M HCl in the presence and absence of inhibitors BI_1 and BI_2 at 298 K, SEM figures were obtained via using FEI quanta 200 scanning electron microscope.

3. Results and discussion

3.1. Effect of tested inhibitors concentration

3.1. 1. Weight-loss-tests

Steel samples are immersed in 1 M HCl solution at various contents of BI_1 and BI_2 during 6 h at 298 K. The values of the corrosion rate (W_{corr}) and inhibition efficiency were given in Table 1. The inhibition efficiency (E_w%) was determined from the relationship(1):

$$E_W\% = \left(1 + \frac{W_{corr}^{inh}}{W_{corr}^{\circ}}\right) \times 100 \qquad (1)$$

W_{corr}^{inh} and W_{corr}° are the weight loss of steel with and without the inhibitor, respectively.

Table1. Gravimetric results of steel corrosion in 1M HCl in the presence of benzimidazolone compounds after 6h of immersion time.

Inhibitor	Concentration (mol/l)	W_{corr}. (mg $cm^{-2}h^{-1}$)	Efficiency (%)	Surface recovered θ
HCl 1M	**00**	**0,313**		
BI1	**10^{-3}**	**0,026**	**91,5**	**0,915**
	10^{-4}	**0,045**	**85,6**	**0,856**
	10^{-5}	**0,065**	**79,0**	**0,79**
	10^{-6}	**0,137**	**56,0**	**0,56**
BI2	**10^{-3}**	**0,011**	**96,6**	**0,966**
	10^{-4}	**0,043**	**86,0**	**0,86**
	10^{-5}	**0,098**	**68,5**	**0.685**
	10^{-6}	**0,158**	**49,4**	**0,494**

The added molecules exhibit an inhibitive effect on the corrosion of steel in molar hydrochloric acid solution. Inhibition efficiency increases with BI_1 and BI_2 content to attain 91, 5% and 96,6 % at 10^{-3} M, respectively. This behavior could be attributed due to strong interaction of compounds with the metal surface that results in the adsorption of inhibitor molecules **[6].** Generally, the effectiveness of a compound as a corrosion inhibitor depends on the structure of the organic compound. It is apparent from the molecular structures that these

compounds are able to get adsorbed on the metal surface through π electrons of aromatic ring and lone pair of electrons of N- and O-atom, and as a protonated species like various amines **[2].**
The difference obtained in inhibiting efficiency may be explained by increasing of effective electron density of the inhibitor BI_2, which can be due to the presence of additional π bond in allyl group.

3.1.2. Potentiodynamic polarization studies

Polarization curves, obtained in the presence and absence of BI_1 and BI_2, after prepolarizing the electrode at its E_{corr} for 30 mn, are shown in **Figure 2.** The potential was swept stepwise from the most cathodic potential to the anodic direction.

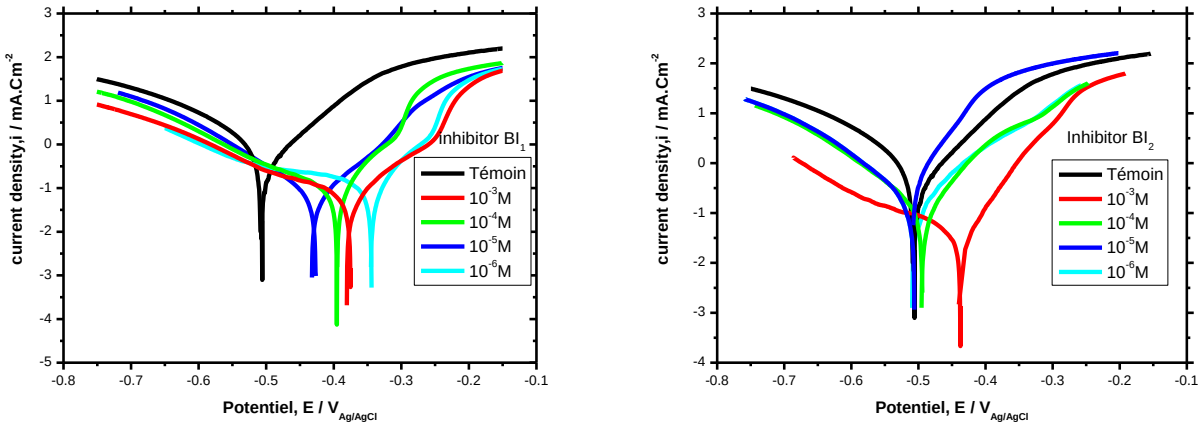

.

Fig. 2: Polarization curves for mild steel in 1 M HCl at various concentrations of BI_1 and BI2 respectively.

Figure.2. shows typical polarization curves for the inhibiting characteristics of benzimidazolone compounds studied, this figure shows that the cathodic current-potential curves give rise to Tafel lines, indicating that the inhibitors are first adsorbed onto iron surface and therefore impedes by merely blocking the actives sites of hydrogen evolution reaction without affecting the cathodic reaction mechanism **[15].** In anodic domain, the addition of inhibitors leads a decrease in the current densities in large potential domain. It is also observed that for potential higher than -0,25$V_{Ag/AgCl}$, the inhibitors start to be desorbed which means that in this case the significant steel dissolution dominates the adsorption of inhibitors **[17-18]**, therefore in the vicinity of E_{corr}, an appreciable decrease in current density is observed especially for BI_1. This phenomenon reflects the formation of anodic protective film on the electrode surface.
As it can be seen from **Figure 2**, the addition of 1, 3-dihydro-2H-benzimidazol-2-one (BI_1) induced a marked decrease in the anodic and a slight decrease in the cathodic current densities. Accordingly, this inhibitor affects slightly the hydrogen reaction discharge and affects greatly the mild steel dissolution process. Moreover, the corrosion potential is shifted into anodic direction in the presence of different concentration. In contrast, The addition of 1-(prop-2-en-1-yl)-1,3-dihydro-2H-benzimidazol-2-one (BI_2) to acid solution shifts both the anodic and cathodic branches to lower values of current density at all concentration, which could be due to an increase of the energy barrier for anodic mild steel dissolution and the hydrogen proton discharge **[13].** Beside, BI_2 have no definite trend in the shift of corrosion potential values except at higher concentration which is shifted slightly into anodic potential.
This result suggests that BI_1 is considered mainly as an inhibitor of predominant anodic effect, while BI_2 acts essentially as mixed-type inhibitor in the range of concentration from 10^{-6}M to 10^{-4}M with predominant control of anodic reaction at 10^{-3} M of this inhibitor.

Table 2 exemplifies The electrochemical parameters, i.e. corrosion current density (i_{corr}), potential of corrosion (E_{corr}), cathodic Tafel slope β_C , and inhibition efficiencies (E_{I-E}%)
The inhibition efficiency of the inhibitors was evaluated using the relationship (2)

$$E\%_{\,I-E} = \frac{i^0_{corr} + i_{corr}}{i^0_{corr}} \times 100 \qquad (2)$$

i_{corr} and i^0_{corr} are the corrosion current densities values without and with inhibitors, respectively, Determined by extrapolation of cathodic Tafel lines to the corrosion potential.

Table 2: Electrochemical parameters of iron in 1 M HCl , without and with different concentrations benzimidazolone derivatives at 298 K .

	Concentration(M)	E_{corr} ($mV_{Ag/AgCl}$)	I_{corr} (µA/Cm)	| βc | (mV dec^{-1})	$E\%_{I-E}$
	HCl 1M	**-521.3**	**1027**	**173.5**	
product BI_1	**10^{-3}**	**-375.1**	**74.3**	**219.5**	**92.7**
	1.10^{-4}	**-395.3**	**108.7**	**192**	**89.4**
	1.10^{-5}	**-344.1**	**175.2**	**153.4**	**89**
	1.10^{-6}	**-426.7**	**186.4**	**134.8**	**81.8**
Product BI_2	**1.10^{-3}**	**-437.3**	**40.5**	**195.1**	**96**
	1.10^{-4}	**-493.6**	**170.2**	**118.8**	**83.4**
	1.10^{-5}	**-494.8**	**160.2**	**112.14**	**84.4**
	1.10^{-6}	**-506.2**	**265.7**	**122.6**	**74.12**

The experimental data shows that i_{corr} values decreases gradually with the increase in concentration of both inhibitors. Beside, the inhibition efficiencies increases with inhibitor concentration reaching the values of 92,7 % and 96 % at 10^{-3} M of BI_1 and BI_2, respectively. Cathodic Tafel slopes β_c, are approximately constant, meaning that the inhibiting action of these molecules occurred by simple blocking of the available surface area; i.e. the inhibitors decreased the surface area for hydrogen evolution without affecting the reaction mechanism **[19].**

3.1.3. Electrochemical impedance spectroscopy (EIS)

To confirm the obtained results by potentiodynamic polarization curves, and study the inhibition mechanism in more detail, the effects of benzimidazolone compounds concentrations on the impedance behavior of mild steel in 1M HCl solution have been studied. The EIS measurement was performed under potentiostatic conditions at E_{corr} in the range of 100 kHz to 10 mHz. Representative Nyquist diagrams in inhibited and uninhibited solutions containing different concentrations of BI_1 and BI_2 are shown in **figure 3.**
The impedance diagrams obtained show a typical set of Nyquist plots for mild steel in 1 M HCl medium with and without various concentrations of benzimidazolone compounds. As it can be observed from these plots, the curves acquired are not perfect semicircles and this difference has been attributed to frequency dispersion **[26-28]**, this phenomenon is generally attributed to different physical processes such as the no homogeneity of the electrode surface or its roughness during the corrosion process **[29-32].**
It is apparent from these spectra that the impedance response of mild steel has significantly changed after the addition of benzimidazolone derivatives in the corrosive medium. Indeed the impedance of inhibited electrode increases with increasing inhibitors concentration.

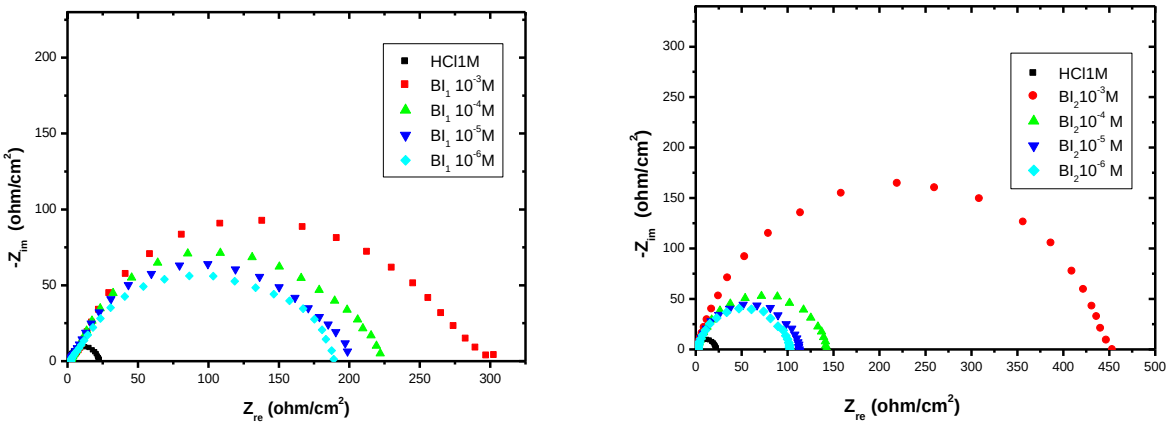

Fig. 3: Nyquist plots of steel in 1M HCl containing various concentration of inhibitor BI_1 and BI_2**.**

Table 3 summaries the characteristic kinetic parameters associated to the impedance study such as the charge-transfer resistance R_{ct}, the double layer capacitance C_{dl} and the inhibiting efficiency E_{Rct} %.
The charge-transfer resistance (R_{ct}) values are calculated from the difference in impedance at lower and higher frequencies **[33].** Whereas, the double layer capacitance (C_{dl}) and the frequency at which the imaginary component of the impedance is maximal (-Zmax) are found as represented in equation (**Eq. 4**).

$$C_{dl} = \frac{1}{\omega R_{ct}} \quad \text{Where} \quad \omega = 2\pi f_{max} \qquad (4)$$

The percentage inhibiting efficiency obtained from the charge-transfer resistance was calculated as follows

$$E\%_{Rct} = \frac{R_{ct/inh} - R_{ct}}{R_{ct/inh}} \times 100 \qquad (5)$$

Where R_{ct} and $R_{ct/inh}$ are the charge-transfer resistance values with and without inhibitor, respectively.

Table 3: EIS data of mild steel in 1 M HCl containing different concentrations of the studied inhibitors at 298 K

	Concentration	R_t (Ω Cm^2)	F_{max} (Hz)	C_{dl}(µF)	E_{Rct} %
HCl	**1M**	**22.6**	**55.37**	**127**	**-**
Inhibitor BI_1	**10^{-3}**	**298.5**	**2.35**	**227**	**92.4**
	1.10^{-4}	**232.5**	**2.35**	**291.4**	**90.2**
	1.10^{-5}	**195.7**	**3.35**	**345.7**	**88.5**
	1.10^{-6}	**187**	**2.34**	**363.5**	**87.9**
Inhibitor BI_2	**1.10^{-3}**	**468**	**5.18**	**65.68**	**95**
	1.10^{-4}	**150**	**11.42**	**92.9**	**84.9**
	1.10^{-5}	**114**	**11.42**	**122.3**	**80**
	1.10^{-6}	**104**	**11.42**	**134**	**78.2**

The inhibition efficiencies calculated from EIS (**Table 3**), showed the same trend as those obtained from potentiodynamic polarization plots. The addition of inhibitors to HCl is found to enhance R_{ct} values and bring down C_{dl} values. These observations clearly bring out the fact that the corrosion of mild steel in 1M HCl is

controlled by a charge transfer process and the inhibition of corrosion occurs through the adsorption of benzimidazolone derivatives molecules on the mild steel surface **[34].**
The same effect has been observed by Chetouani et al. for the study of pyrazolic derivatives **[35].**

3.2. Effect of temperature

The temperature can modify the interaction between the steel electrode and the acidic medium in the absence and presence of the inhibitors. In order to gain more information about the adsorption type and the performance of the investigated inhibitors at higher temperatures, weight loss measurements are being employed with the range of temperature 303, 313, 323 and 333K for 2 h of immersion time at different concentrations of investigated inhibitors . Results obtained are given in **table 4.**

Table 4: Influence of temperature on the corrosion rate of mild steel in the presence and absence of inhibitors BI_1 and BI_2 at various concentration for 2h immersion time.

Temperature (k)	**Concentration (Mol/L)**	**Inhibitor BI_1**		**Inhibitor BI_2**	
		W_{corr} (mg cm^{-2} h^{-1})	**E_{inh} %**	**W_{corr} (mg cm^{-2} h^{-1})**	**E_{inh} %**
303	**00**	**0.360**		**0.360**	
	10^{-3}	**0.0475**	**86.8**	**0.0372**	**89.9**
	10^{-4}	**0.097**	**73**	**0.063**	**82.9**
	10^{-5}	**0.258**	**28.2**	**0.116**	**68.4**
	10^{-6}	**0.302**	**15.9**	**0.188**	**48.9**
313	**00**	**1.120**		**1.120**	
	10^{-3}	**0.1355**	**87.9**	**0.112**	**90**
	10^{-4}	**0.288**	**74.2**	**0.204**	**81.4**
	10^{-5}	**0.904**	**19.2**	**0.454**	**59.4**
	10^{-6}	**0.969**	**13.4**	**0.773**	**31**
323	**00**	**1.49**		**1.49**	
	10^{-3}	**0.193**	**87**	**0.146**	**90.2**
	10^{-4}	**0.417**	**72**	**0.283**	**81**
	10^{-5}	**1.102**	**26**	**0.551**	**63.9**
	10^{-6}	**1.311**	**12**	**1.07**	**28**
333	**00**	**3.07**		**3.07**	
	10^{-3}	**0.371**	**87.9**	**0.294**	**90.4**
	10^{-4}	**0.89**	**71**	**0.614**	**80**
	10^{-5}	**2.51**	**18.2**	**1.66**	**64.2**
	10^{-6}	**2.686**	**12.5**	**2.68**	**12.7**

As it can be observed, the corrosion rates increase with temperature. This increase is much more pronounced in uninhibited than in inhibited media. Therefore, the values of inhibition efficiencies of BI_1 and BI_2 remain constant with temperature increase at 10^{-3} M concentration, indicating that the inhibitive film formed on the metal surface is protective in nature at higher temperatures. But for inhibitors concentrations lower than 10^{-3} M corrosion rate decrease markedly with increasing temperature as a result of the higher dissolution of mild steel at higher temperature, which might cause the desorption of investigated inhibitors from the mild steel surface **[36].**

3.2.1. Thermodynamic parameters of the activation corrosion process

Activation parameters like activation energy (E_a), enthalpy (ΔH^*), and entropy (ΔS^*) for the dissolution of mild steel in 1 M HCl in the absence and presence of various concentrations of BI_1 and BI_2 were calculated from the Arrhenius equation (Eq.7) and its alternative formulation called transition state equation (Eq. 8) **[37-38]:**

$$W_{corr} = A exp(\frac{-E_a}{RT}) \quad (7)$$

$$W_{corr} = \frac{k_B T}{h} \exp(\frac{\Delta S^*}{R}) \exp(-\frac{\Delta H^*}{RT}) \quad (8)$$

Where W_{corr} is the corrosion rate, A is the Arrhenius pre-exponential constant, E_a is the activation energy for the corrosion process, k_B is the Boltzmann's constant (k_B = 1.38066 10^{-23} $J.K^{-1}$), h is the Planck's constant (h = 6.6252 10^{-34} J.s), ΔH^* and ΔS^* are the activation enthalpy and the entropy activation of corrosion process, respectively.

Figure 6 presents the Arrhenius plots of the weight-loss versus 1/T, for mild steel in the corrosive medium with and without addition of BI_1 and BI_2 respectively, at different concentrations. Straight lines are obtained with a slope of ($-E_a/R$). **Figure 7** shows the plot of Ln (W_{corr}/T) against 1/T. Straight lines are obtained with a slope of ($\Delta H^*/R$) and an intercept of ($Lnk_B/+ \Delta S^*/R$), which give the values of ΔH^* and ΔS^*.

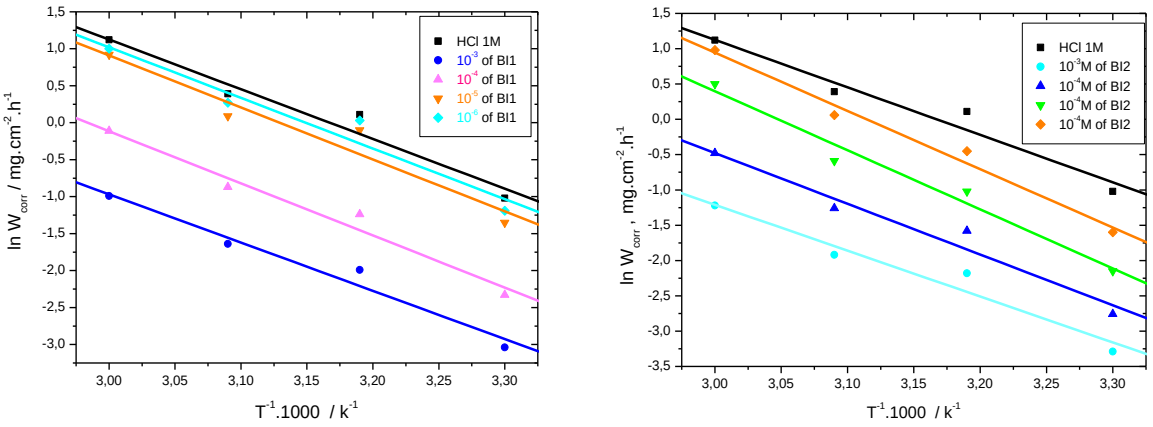

Fig. 6: Arrhenius plots of $\ln W_{corr}$ versus 1/T at various concentrations of BI_1 and BI_2

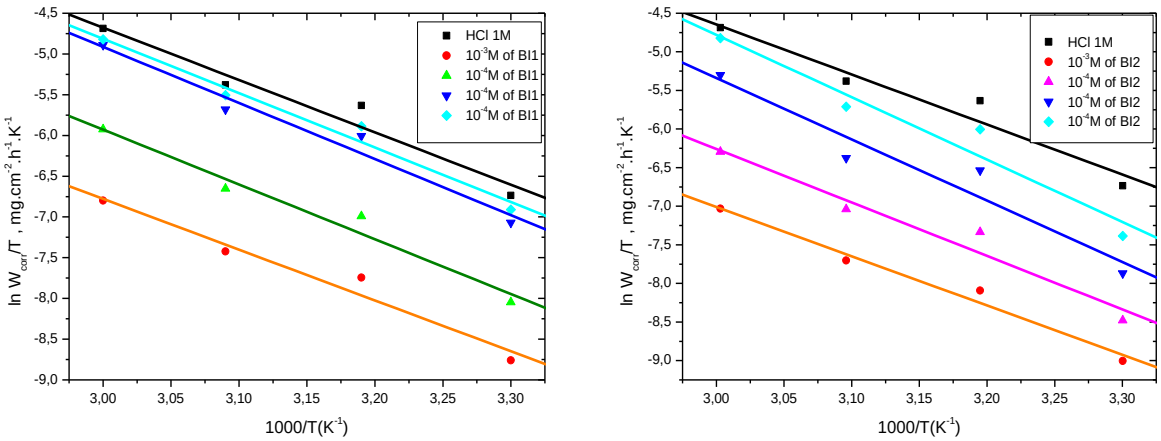

Fig. 7: Arrhenius plots of $\ln W_{corr}$ /T versus 1/*T* at various concentrations of BI_1 and BI_2

All the linear regression coefficients R^2 are close to 1, indicating that the steel corrosion in inhibited and uninhibited media can be elucidated using the kinetic model. **Table 5** shows the values of activation parameters (Ea, ΔH^* and ΔS^*) for mild steel in the corrosive medium at different concentrations of BI_1 and BI_2.

Table 5: Activation parameters E_a, ΔH^* and ΔS^* of mild steel dissolution in 1 M HCl in the absence and in the presence of BI_1 and BI_2 at different concentrations.

Inhibitors	**Concentration (mol/L)**	**Pre-exponential factor, A (mg $cm^{-2}h^{-1}$)**	**E_a (kJ .mol^{-1})**	**ΔH^* (kJ .mol^{-1})**	**ΔS^* (kJ .$mol^{-1}.K^{-1}$)**
	00	$1.78.10^9$	55.9	53.4	**-75.7**
BI_1	10^{-3}	$1.21.10^8$	54.2	51.8	-101.6
	10^{-4}	$1.36.10^9$	58.6	55.9	-78.5
	10^{-5}	$3.55.10^9$	58.4	57.2	-46.4
	10^{-6}	$4.05.10^9$	58.3	55.5	-37.6
BI_2	10^{-3}	$8.71.10^8$	54	52.6	-97.2
	10^{-4}	$1.42.10^9$	59.7	57	-81.4
	10^{-5}	$6.39.10^{10}$	76.8	65.4	-70.5
	10^{-6}	$5.34.10^8$	64	66.6	-113.6

The temperature dependence of the inhibiting effect and the comparison of the values of the apparent activation energy of the corrosion process in the absence and presence of inhibitors can provide further evidence **[25, 26].** Concerning the mechanism of the inhibiting action, the lower value of E_a in inhibited solution when compared to that for uninhibited one show that strong chemisorption bond between the inhibitor and the metal is highly probable. In the opposite case a physisorption can usually occur **[27].** From Table 5, it appears that the apparent activation energy values in inhibited medium are slowly lower than the one in the blank solution at the concentration 10^{-3}M. whereas for concentrations lower than 10^{-3} M Ea values are greater than that in 1 M HCl. The variation of Ea, with the inhibitor's concentration increase, from a greater to a lower value than that in an uninhibited solution is ascribed in Ref. **[30]** to the physical adsorption transition to chemisorptions. Riggs **[31]** considers the rate of metal dissolution in presence of an inhibitor as a sum of two rates: the first one is connected with the process taking place on the surface free from an inhibitor, while the second one with that proceeding on the surface occupied by the inhibitor. At high concentrations the first rate is insignificantly small and the corrosion mechanism includes a direct reaction of the inhibitor molecules with the surface of the metal. Then the Ea of the inhibited metal dissolution can be higher as well as lower than that of the uninhibited reaction in case of a high degree of surface coverage. Hence, it can be suggested that the adsorption of benzimidazolone onto mild steel surface can involve both physisorption and chemisorptions. The positive values of ΔH^* mean that the dissolution reaction is an endothermic process and that the dissolution of steel is difficult **[33].** Practically Ea and $\Delta H^*$are of the same order. On the other hand, the entropy ΔS^* increases negatively in the presence of BI_1 and BI_2 with increasing of inhibitor concentration. This reflects the formation of an ordered stable layer of these inhibitors onto the mild steel surface electrode **[39].**

3.2.2. Thermodynamic parameters of the adsorption process

Basic information dealing with interaction between inhibitor molecules and the metal surface can be provided by adsorption isotherms. The adsorption process of inhibitor is a displacement reaction where the adsorbed water molecule is being removed from the surface of metal **[36]:**

$$Org\ (sol) + n\ H_2O\ (ads) \rightarrow Org\ (ads) + H_2O\ (sol)$$

Org (sol) and Org (ads) are the organic molecules in the aqueous solution that adsorbed to the metal surface. While H_2O (ads) is the water molecule on the metal surface in which n is the coefficient that represents water molecules replaced by a unit of inhibitor. Four types of adsorption may take place by organic molecules at the metal/solution interface: (1) electrostatic attraction between the charged metal and the charged molecules, (2) interaction of uncharged electrons pair in the molecule with the metal, (3) interaction of Tapez une équation ici. electrons with the metal and (4) combination of (1 and 3) **[18].**

The surface coverage values (θ) were evaluated by corrosion rate obtained from weight loss method. The (θ) values for different inhibitor concentrations were tested by fitting to various isotherms. The best fit was obtained with Langmuir isotherm (Fig. 8). According to this isotherm, the surface coverage θ is related to the equilibrium adsorption constant K_{ads} and concentration of inhibitor C via **[34]:**

$$\frac{C}{\theta} = \frac{1}{K_{ads}} + C_{inh} \qquad (9)$$

Where C_{inh} is the inhibitor concentration, K_{ads} is equivalent constant and θ is the surface coverage. The free adsorption energy is calculated from the equilibrium adsorption constant:

$$\Delta G^0_{ads} = -RT\ ln55{,}55\ K_{ads} \qquad (10)$$

Where ΔG^0_{ads} is the free energy adsorption and the value of 55,55 in the above equation is the concentration of water in solution in mol L^{-1}

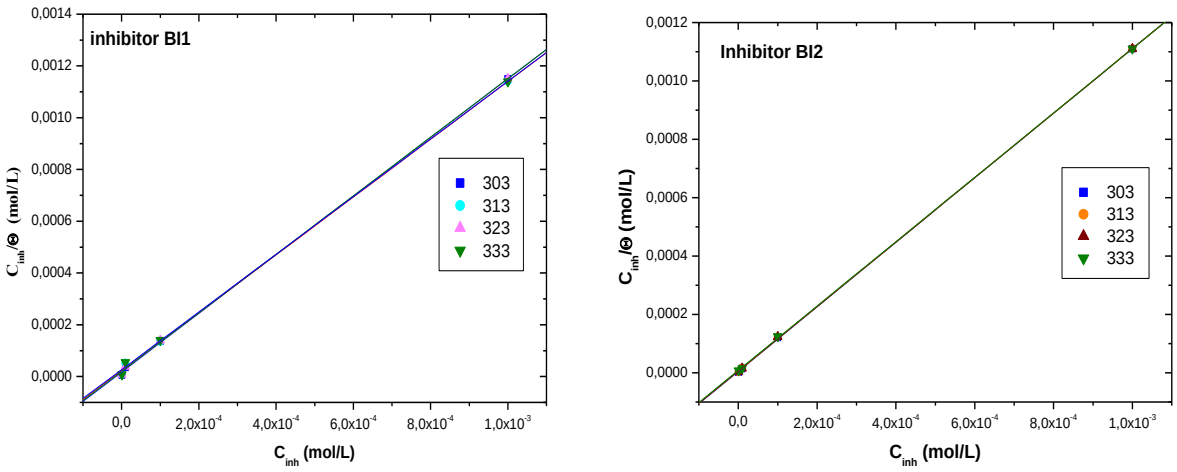

Fig. 8: Langmuir adsorption plots for mild steel in 1 M HCl solution containing different concentration of BI_1 and BI_2 at different temperature.

The Langmuir isotherm was found to provide the best description of the adsorption behavior. The plots of C_{inh}/θ versus C_{inh} (**Fig. 8**) with slopes around unity, and regression coefficients, R^2, almost equal to 1 suggests that inhibitors tested in present study obeyed the Langmuir isotherm, and there is negligible interaction between the adsorbed molecules.

From the intercepts of the straight lines C_{inh}/θ axis, K_{ads} values were calculated. The standard free energy of adsorption ΔG^0_{ads} ensures the spontaneity of adsorption process and stability of the adsorbed layer on the steel surface.

The thermodynamics parameters derived from Langmuir adsorption isotherms for the studied compounds, are given in **Table 6.** The negative values of ΔG^0_{ads} indicate a spontaneous adsorption process also; the high K_{ads} values reflect the high adsorption ability of these inhibitors on the metallic surface [**30].** Generally, the standard free energy of adsorption values of - 20 kJ mol^{-1} or less negative are associated with an electrostatic interaction between charged molecules and charged metal surface ; physisorption; those of -40 kJ mol^{-1} or more negative

involve charge sharing or transfer from the inhibitor molecules to the metal surface to form a coordinate covalent bond, chemisorption **[31,32].**

Table 6: Thermodynamic parameters for the adsorption of BI_1 and BI_2 in HCl on steel at different temperatures.

Inhibitors	Temperature (K)	Adsorption constant K_{ads}	ΔG^0_{ads} (kJ/mol)	ΔH^0_{ads} (kJ/mol)	ΔS^0_{ads} (kJ/mol.k)
BI1	303	$5.73.10^4$	-37.7	-11.4	6.9
	313	$4.86.10^4$	-38.5		
	323	$4.41.10^4$	-39.5		
	333	$3.76.10^4$	-40.3		
BI2	303	$2.09.10^5$	-41.0	-14.2	6.92
	313	$1.51.10^5$	-41.5		
	323	$1.58.10^5$	-42.9		
	333	$1.17.10^5$	-43.4		

The values of ΔG^0_{ads} in our measurements range from -37 to -40 kJ mol^{-1} for BI_1, indicate that the adsorption of this inhibitor involves two types of interaction, chemisorption and physisorption. But more negative values obtained for BI_2 suggest that the adsorption mechanism of BI_2 is generally made by chemisorptions rather than by physisorption.
The corrosion inhibition for mild steel may be well explained by using a thermodynamic model, so, the heat, the free energy and the entropy of adsorption are calculated to elucidate the phenomenon for the inhibition action of BI_1 and BI_2 **(Table 7)**. According to the Van't Hoff equation (Eq.11) **[40]:**

$$\ln K_{ads} = -\frac{\Delta H^0_{ads}}{RT} + cte \qquad (11)$$

Figure 9 shows the plot of ln K_{ads} versus *1/T*. It gives straight line with slope of ($-\Delta H^0_{ads}/R$) and an intercept of ($\Delta S^0_{ads}/R$ –ln55,55) when considering a combination of equation 10 and the thermodynamic equation 12:

$$\Delta G^0_{ads} = \Delta H^0_{ads} - T\Delta S^0_{ads} \qquad (12)$$

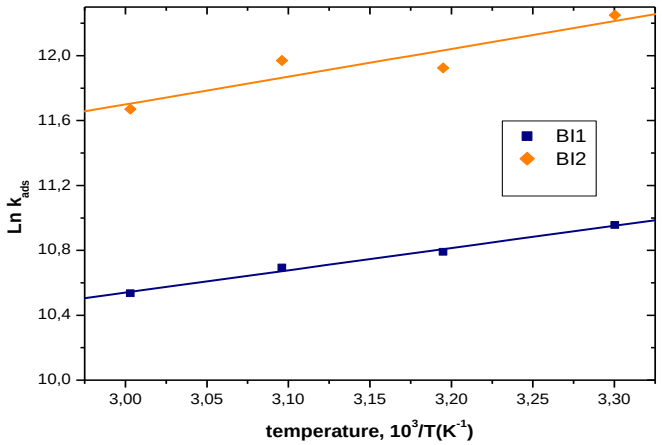

Fig. 9: Vant'Hoff isobar plot for mild steel/BI_1 and BI_2 systems in 1 M HCl.

It is assumed that an exothermic process is attributed to either physical or chemical adsorption but endothermic process corresponds solely to chemisorption. In this study, the values calculated of ΔH_{ads}^{0} for both inhibitors are negatives ($\Delta H_{ads}^{0} = -11{,}4$ kJ /mol and $\Delta H_{ads}^{0} = -14{,}2$ kJ/ mol) for BI_1 and BI_2 respectively, reflecting the exothermic behaviour of adsorption on the steel surface. The negative values of ΔS_{ads}^{0} ads is generally explained by an ordered of adsorbed molecules of inhibitor with the progress in the adsorption onto the mild steel surface **[40].** Values of ΔS_{ads}^{0} in the presence of BI_1 and BI_2 (Table 7) are large and positive meaning that an increase in disordering takes places in going from reactants to the metal-adsorbed species reaction complex **[41].** It is to be noted that values of ΔH_{ads}^{0} and ΔS_{ads}^{0} derived from the plot of ΔG_{ads}^{0} /T vs. 1/T are very comparable to those obtained from the plot ln K_{ads} vs. 1/T

4. Scanning Electron Microscopy (SEM)

Surface analyses for the corrosion of mild steel specimens in 1M HCl solution without and with inhibitors were carried out by SEM. **Figure 10** and **11** represent the scanning electron microscopic (SEM) images of mild steel surface that has been exposed to the 1M HCl for 6h in the absence and presence of studied inhibitors, respectively.

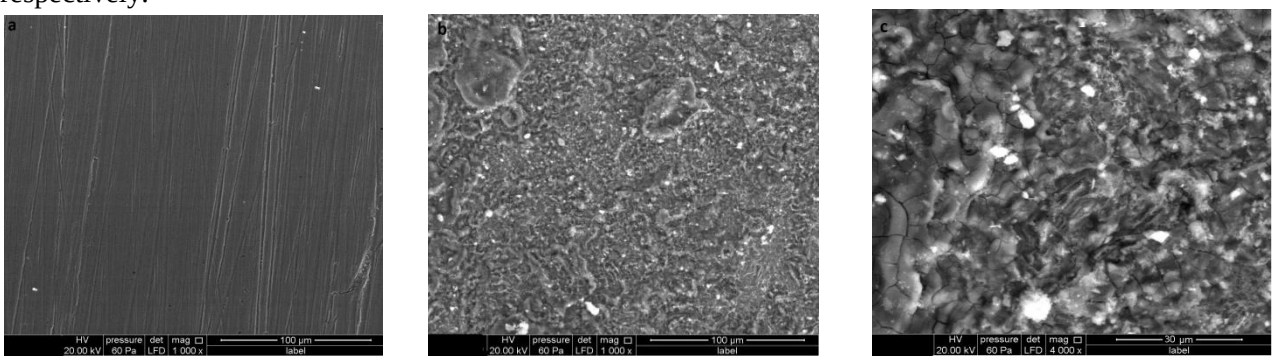

Fig. 10: SEM image of mild steel surface (a) before immersion in 1M HCl, (b) and (C) after 6 hours of immersion in 1M HCl solution in the absence of inhibitors.

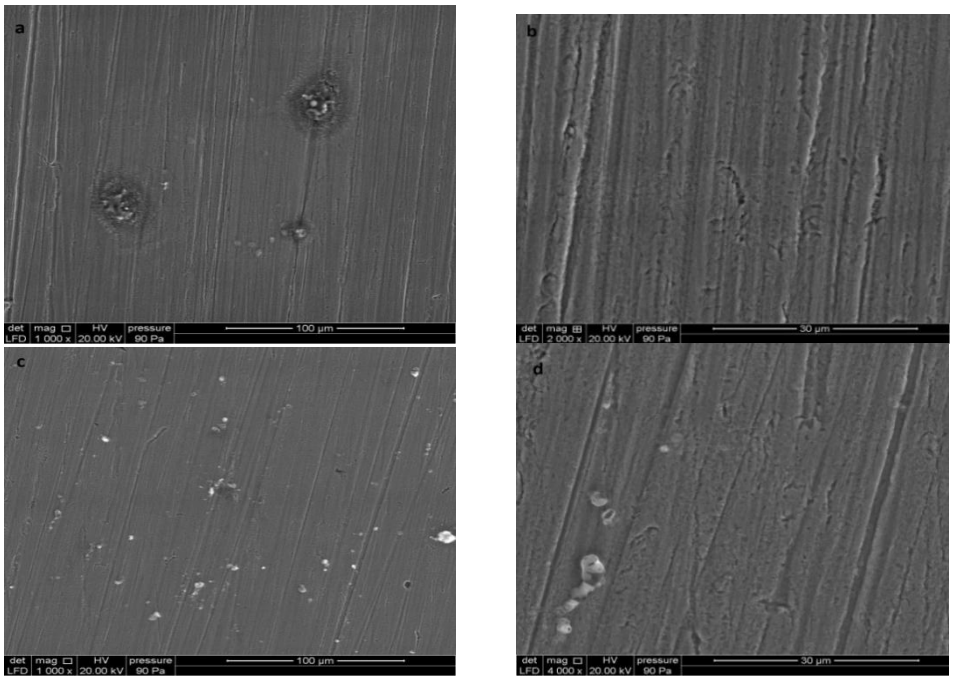

Fig. 11: SEM image of mild steel after 6 hours of immersion in 1M HCl solution: (a) and (b) with 10^{-3} M of inhibitor BI_1 ; (b) and (C) with 10^{-3} M of inhibitor BI_2.

The morphology of surface in the presence of HCl 1M shows that the steel sample is seriously damaged by the corrosive solution (fig 10: b and c). Indeed, EDAX analysis **(Fig.12**) furthers identified characteristic corrosion products (elements of Fe, O and C).

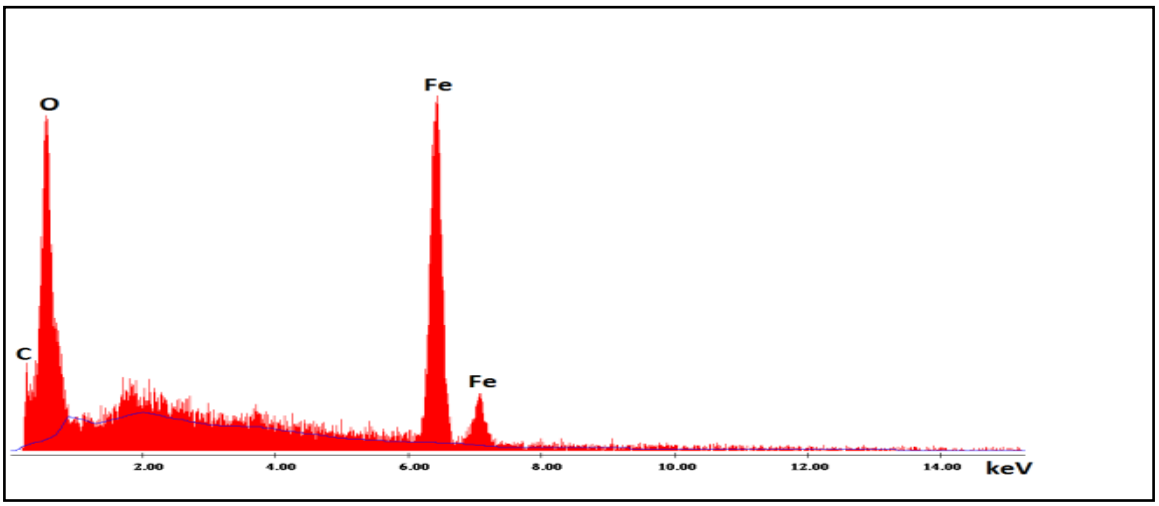

Fig.12: EDAX profile of mild steel surface after 6h of immersion in HCl 1M solution in the absence of inhibitors BI_1 and BI_2.

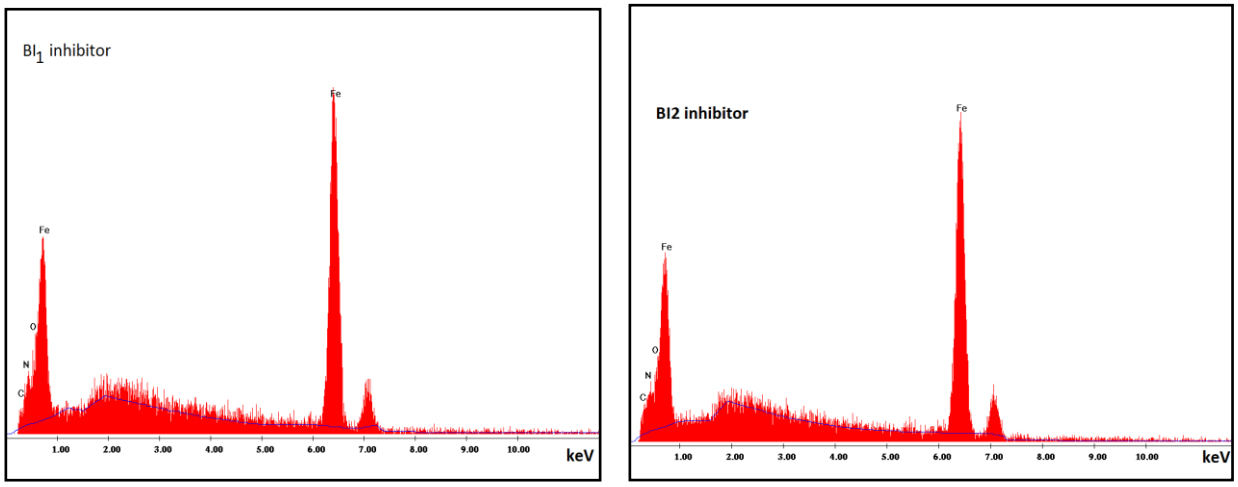

Fig.13: EDAX profile of mild steel surface after 6h of immersion in HCl 1M solution in the presence of inhibitors BI_1 and BI_2 respectively.

Furthermore, the SEM image in the presence of both BI_1 and BI_2 inhibitors (**Fig. 11**) shows a large area free from corrosion and scale products. It reveals that this is a good protective film adsorbed on specimen surface which is responsible for the inhibition of corrosion. In this case, EDAX analysis (**Fig. 13**) shows lowest X-ray intensity value of carbon and oxygen as compared with inhibitor-free solution indicating the molecule of inhibitors are adsorbed on the metallic surface. Also EDAX analysis (**Fig.13**) shows the appearance of nitrogen band for both inhibitors indicating that the benzimidazolone studied may be adsorbed onto the surface of mild steel via electrons pairs of the nitrogen heteroatom.

Conclusion

Results obtained show that benzimidazolone derivatives tested are good inhibitors of mild steel in 1M HCl.

- The inhibition efficiency of the studied inhibitors increased with inhibitor concentrations.
- Potentiondynamic polarization measurements show that BI_1 act as anodic-type inhibitor whereas, BI_2 act essentially as mixed-type inhibitor with anodic predominance at 10^{-3} M.
- EIS measurements shows that the use of BI_1 and BI_2 significantly increases the charge transfer values and decreases the double layer capacitance in 1M HCl, suggesting that the corrosion inhibition takes place by simple adsorption.
- The weight loss, electrochemical impedance spectroscopy and polarisation curves were in good agreement.
- The adsorption of investigated inhibitors on the mild steel surface follows the Langmuir adsorption isotherm. The free energy of adsorption ΔG_{ads}, indicates that the process was spontaneous.
- The confrontation of various thermodynamic parameters of activation corrosion process and adsorption process indicate that benzimidazolone derivatives studied are adsorbed, by mixed mode (physisorption and chemisorptions both involved to some extent) onto the mild steel surface.
- Scanning electron microscopy shows a smoother surface for inhibited metal sample than uninhibited samples due to the formation of film like deposit on the inhibited surface.

References

1. Zerga B., Saddik R., Hammouti B., Taleb M., Sfaira M., Ebn Touhami M., Al-Deyab S.S., Benchat N., *Int. J. Electrochem. Sci*., 7 (2012) 631.
2. El-Hajjaji F., Zerga B., Sfaira M., Taleb M., Ebn Touhami M., Hammouti B., Al-Deyab S.S., Benzeid H. El M. Essassi,*J. Mater. Environ. Sci.*, 5 (2014) 255.
3. Guendouz *A*., Missoum N., Chetouani A., Al-Deyab S. S, Ben Cheikhe B., Boussalah N., Hammouti B., Taleb M., Aouniti A., *Int. J. Electrochem. Sci.*, 8 (2013) 4305
4. Aloui S., Forsal I., Sfaira M., Ebn Touhami M., Taleb M., Filali Baba M., Daoudi M., *Portug. Electrochim. Acta*, 27 (2009) 599.
5. Aljourani J., Golozarm K., Raeissi M.A., *J. Materials chemistry and physics*, 121 (2010) 320-325
6. Elkacimi Y., Achnin M., Aouine Y., Ebn Touhami M., Alami A., Touir R., Sfaira M., Chebabe D., Elachqar A., Hammouti B.,*Portug. Electrochim. Acta*, 30 (2012) 53.
7. Aouine Y., Sfaira M., Ebn Touhami M., Alami A., Hammouti B., Elbakri M., El Hallaoui A., Touir R., *Int. J. Electrochem. Sci*., 7 (2012) 5400.
8. Zerga B., Hammouti B., Ebn Touhami M., Touir R., Taleb M., Sfaira M., Bennajeh M., Forssal I., *Int. J. Electrochem. Sci.*, 7 (2012) 471.
9. El Adnani Z., Mcharfi M., Sfaira M., Benjelloun A.T., Benzakour M., Ebn Touhami M., Hammouti B., Taleb M., *Int. J. Electrochem. Sci*., 7 (2012) 3982.
10. El Khattabi O., Zerga B., Sfaira M., Taleb M., Ebn Touhami M., Hammouti B., Herrag L., Mcharfi M., *Der. Phar. Chem*., 4 (2012) 1759.
11. Zerga B., Saddik R., Hammouti B., Taleb M., Sfaira M., Ebn Touhami M., Al-Deyab S.S., Benchat N., *Int. J. Electrochem. Sci*., 7 (2012) 631
12. Zerga B., Attayibat A., Sfaira M., Taleb M., Hammouti B., Ebn Touhami M., Radi S., Rais Z., *J. Appl. Electrochem.*, 40 (2010) 1575.
13. Xiumei Wang, Ye Wan, You Zeng, Yaxin Gu, *Int. J. Electrochem. Sci.*, 7 (2012) 2403
14. Bouckamp A.: *Users Manual Equivalent Circuit*, Ver. 4.51 (1993)
15. Abdel-Rehim S.S., Magdy A.M., Khaled K.F., *J. Appl. Electrochem*. 29 (1999) 593.

16. Popova A., Sokolova E., Raicheva S., Christov M., *Corrosion Science* 45 (2003) 33
17. Bouklah M., Ouassini K., Hammouti B., Elidrissi A., *Appl. Surf. Sci.*, 250 (2005) 50-56.
18. Prasanna B.M., Praveen B.M., Hebbar N., Venkatesha T.V. ; *Mor. J. Chem.*, 3 (2015) 824-837.
19. Chaudhary R.S., Sharma S., *Indian J. Chem. Technol*. 6 (1999) 202
20. Zarrouk A., Warad I., Hammouti B., Dafali A., Al-Deyab S.S., Benchat N., *Int. J. Electrochem. Sci.*, 5 (2010) 1516 – 1526.
21. Gunasekaran G., Chauhan L.R., *Electrochim. Acta* 49 (2004) 4387.
22. Ismaily Alaoui K., El Hajjaji F. , Azaroual M. A., Taleb M., Chetouani A., Hammouti B., Abrigach F., Khoutoul M., Abboud Y., Aouniti A. and Touzani R. , *J. Chem. Pharm. Res.* , 6 (2014) 63
23. Bentiss F., Lagrenée M., Traisnel M., Mernari B. and Elattari H., *J. Appl. Electrochem*. 29 (1999) 1073.
24. Tang Y., Zhang F., Hu S., Cao. Z., Wu Z., Jing W., *corrosion science* 74 (2013) 271
25. Szauer T., Brandt A., *Electrochim. Acta* 26 (1981) 1209.
26. Sfaira M., Srhiri A., Keddam M., Takenouti H., *Electrochim. Acta*, 44 (1999) 4395.
27. Bentiss F., Traisnel M., Genegembre L., Lagrenee M., *Appl. Surf. Sci*. 152, 237 (1999)
28. Duval S., Keddam M., Sfaira M., Srhiri A., Takenouti H., *J. Electrochem. Soc*. 149 (2002) 520.
29. Khaled K.F., *Electrochimica Acta* 48 (2003) 2493
30 Bouklah. M., Benchat N., Aouniti A., Hammouti B., Benkaddour M., Lagrenée M., Vezin H., Bentiss F., *Prog. Org. Coat.* 51 (2004) 118.
31. Riggs O.L., Hurd R.M., *Corrosion* 23 (1967) 252.
32. Juttner K., *Electrochim. Acta* 35 (1990) 1501.
33. Guan N.M., Xueming L., Fei L., *Mater. Chem. Phys*. 86 (2004) 59.
34. Langmuir I., *J. Am. Chem. Soc*. 39 (1947) 1848.
35. Chetouani A., Hammouti B., Benhadda T., Daoudi M., *Appl. Surf. Sci.*, 249 (2005) 375-385.
36. Ozcan M., Dehri I., Erbil M., *Appl. Surf. Sci.* 236 (2004) 155.
37. Popova A., *Corros. Sci.* 49 (2007) 2144
38. Bockris J.O'M., Reddy A.K.N., *Modern Electrochemistry, Plenum Press, New York*, 2 (1977) 1267.
39. Yurt A., Balaban A., Kandemir S.U., Bereket G., Erk B., *Mater. Chem. Phys*. 85 (2004) 420.
40. Do D., Adsorption Analysis: *Equilibria and kinetics, Imperial College Press,* (1980) 10-60.
41. Wang H.-L., Fan H.-B, Zheng J.-S., *Mater. Chem. Phys*. 77 (2002) 655.